PILOT STUDY ON AN ANALYTIC SIZING TOOL APPROACH FOR INSERT LOAD INTRODUCTIONS IN SANDWICH ELEMENTS

J. Wolff[1], M. Brysch[2], C. Hühne[3]

[1] Institute of Composite Structures and Adaptive Systems, German Aerospace Center
Lilienthalplatz 7, D-38108 Braunschweig, Germany
Email: johannes.wolff@dlr.de, Web page: www.dlr.de
[2]Email: marco.brysch@dlr.de, Web Page: www.dlr.de
[3]Email: christian.huehne@dlr.de, Web page: www.dlr.de

Keywords: sandwich, connection, insert, sizing tool, parameter identification

Abstract
Primary design requirements for joints in sandwich structures are weight efficiency and often a removability to serve assembly, repair and replacement demands. Bolted local load introductions on sandwich structures using insert elements provide an excellent load carrying capability. Nowadays a variety of standard insert elements is available, offering a reliable performance even though they are often not optimized in terms of net weight. In the optimization process there is a lack on standard sizing procedures to generate adapted basic insert shapes helping to design lightweight local load introductions. Aim of this work is to investigate fundamental statements which are required for a reliable basis for the tool. This paper presents a study of the mathematical formulation provided by [1] and an investigation of its occasionally large differences compared to experimental results. The uncertainty factors in determining maximal carrying forces are discussed and methods for more precise prediction are presented.

1. Introduction

Sandwich panel structures exhibits an excellent bending stiffness and bending strength to weight ratio. Further benefits are good thermal and acoustic insulation. However, the application of sandwich panels suffers from disadvantages like manufacturing and material costs as well as from higher engineering effort. Therefore, its current application is mostly limited to particular domains such as small series or prototypes of space vehicles, racing cars and military ship super structures [1–10]. The high engineering effort is mainly due to complex failure mechanism and the inability to carry local loads without further construction elements. For this, the aim of this work is to provide an easy to use sizing tool, generate adapted, initial insert geometries as optimal basis for lightweight local load introductions in sandwich panels.
Like in any other mechanical construction, the need to join different parts is necessary in sandwich structures, too. Multiple connection designs are common, ranging from permanent connections by direct [2, 11, 12] or indirect [1, 13] bonding to releasable screw connections [1, 8, 14–17] of sandwich panels (Fig.1). The advantage of removable joints is the ability to meet assembly, rework, repair and disposal demands. Furthermore, an increase of function integration into sandwich elements (like structural supports, cables, pipes, antennas, lighting, grounding and health monitoring systems) can be observed, demanding an easy changeability in case of malfunctions [18–20].

Excerpt from ISBN 978-3-00-053387-7

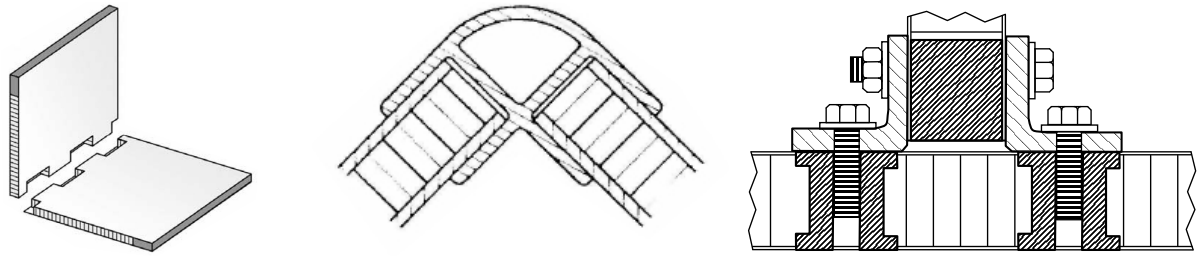

Direct, permanent bonded mortise-and-tenon joint.

Indirect, permanent connection with a bonded plastic or aluminum profile.

Removable, screwed T-connection.

Figure 1. Examples of common permanent and removable sandwich joining methods [21–23])

However, due to the weak core as well as the thin and flexible face sheets, the ability of sandwich elements to carry local loads is very limited. Neither screw clamping nor structural forces can be transferred into the sandwich element directly without causing damage (Fig. 2, top). Hence, unsupported load applications can fail far before the sandwich structure itself, causing an overall weight inefficient structure. For this, multiple supporting methods are common (Fig. 2, down).

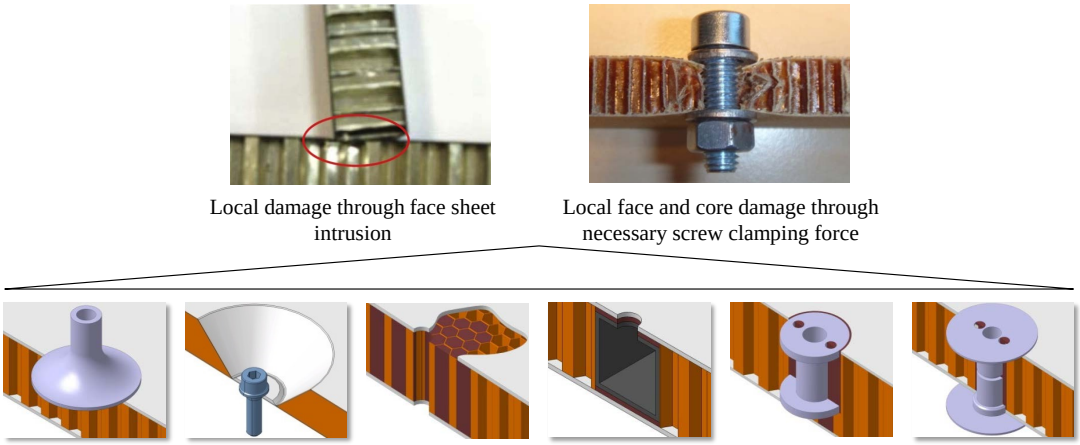

Local damage through face sheet intrusion

Local face and core damage through necessary screw clamping force

Onsert on surface

Joint face sheets (JFS)

Local reinforcement with potting resin

Stabilization by elements

Reinforcement by local insert elements

Figure 2. Supporting elements for load introductions on sandwich elements, (top left by [15]).

In insert load introductions, the cylindrical formed, metallic or plastic insert element stabilizes the core from crushing and introduce the load in the surrounding sandwich structure in a distributed manner. Common insert types feature a wide range of different shapes and integration methods. Insert load introductions can be classified regarding the insert position to the face sheet surfaces (recessed, flush, protruding), the indentation depth of insert and potting resin in the sandwich core (partial, fully, through-the-thickness), (Fig. 3, right side).

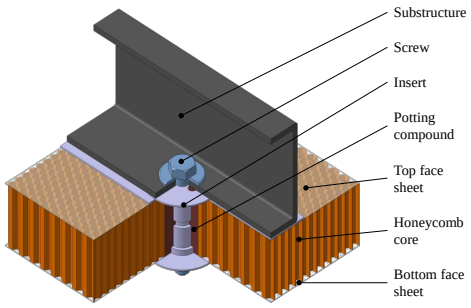

		Indentation depth of insert in honeycomb core		
		Partial potted	Fully potted	Through-the-thickness
Existence of flanges and position regarding the skins	Plane bonded flange, inner side			
	Flush bonded flange			
	Protruding, plane bonded flange			

Figure 3. Notations of an insert load introduction (left), classification of insert types (right).

Excerpt from ISBN 978-3-00-053387-7

Nowadays, standard insert elements are commonly used due to the fact that they are commercially available for a wide bandwidth of different applications. Though, in the design process, standardized insert elements are selected only on basis of empirical data, which minimizes the engineering effort, but means no improvement in terms of mass reduction of the insert load introduction [24–27]. With respect to large constructions like airplane construction or space vehicles with insert connection numbers up to 25,000 units [28], this can make a significant influence to weight and costs, since e. g. launching costs of space vehicles can reach $10K - $50K/kg [15, 29, 30]. Unfortunately, especially for large projects, a further, time consuming engineering effort per particular insert type often cannot be justified. Consequently, there is an urgent need in a standard, straight forward and fast procedure for a basic insert dimension process for lightweight connections.

2. Dimensioning methods for insert elements

For structural applications, [31–33] recommend the use of protruding, through-the-thickness insert types due to their excellent performance in load introductions (Fig. 3, right column). Hence this insert shape will be used as basis for the optimization process exclusively within this work. To allow tolerance compensation in normal direction (respectively a setting of the correct face sheet bonding thickness) and a reduced installation time demand, this basic insert shape embodies a two-component design (Fig. 4).

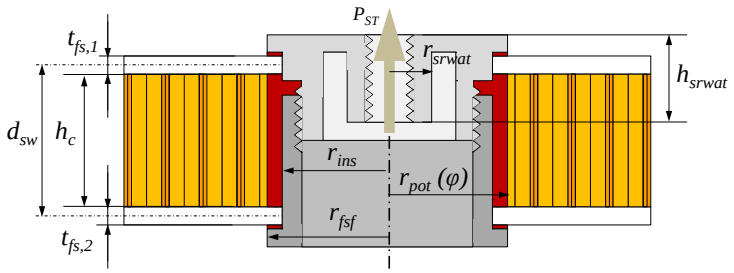

Figure 4. Basic trough-the-thickness insert geometry for the sizing approach.

Recent literature shows three optimization approaches as there are phenomenological approaches, relaying on empirical data generated with tests or numerical methods (finite element analysis) [10, 16, 24, 34–40]), analytic-numeric approaches like the higher order sandwich plate theory (HSAPT) [32, 37, 41–44] or using equations derived from simple analytic-mechanical models refer to the classic sandwich theory [21, 31, 45–47]. Empirical methods and HSAPT methods require sophisticated mathematical effort to optimize individual applications. Therefore, these methods are rather unsuitable in optimizing large numbers of different insert geometries. In contrast, the analytic-mechanical approach provides simple, strait forward analytic relations and therefore is selected for further investigations in this work.
From a mechanical point of view, mass can be saved by reducing the central cylinder radius r_{ins}, the face sheet range radius r_{fsf} and the volume of the screw attachment h_{srwat}, r_{srwat} to their inevitable minima. Analytic algorithms to determine $r_{fsf,min}$ and $r_{ins,min}$ are provided by [8, 21, 31] respectively by [34, 46, 48]. Within this paper, the focus is on the way to determination the minimal central cylinder radius r_{ins}.

3. Mechanical-analytic determination of the minimal insert central cylinder radius r_{ins}

The initial failure mode of insert load introductions which are subjected to transverse load is characterized by shear buckling of single cell-walls next to the potting, see Fig. 5, right. According to [21, 23, 24, 32, 33, 37, 42, 47, 49, 50] and [51], this behavior can be specially observed in sandwich elements with thin (resp. flexural) face sheets.

Excerpt from ISBN 978-3-00-053387-7

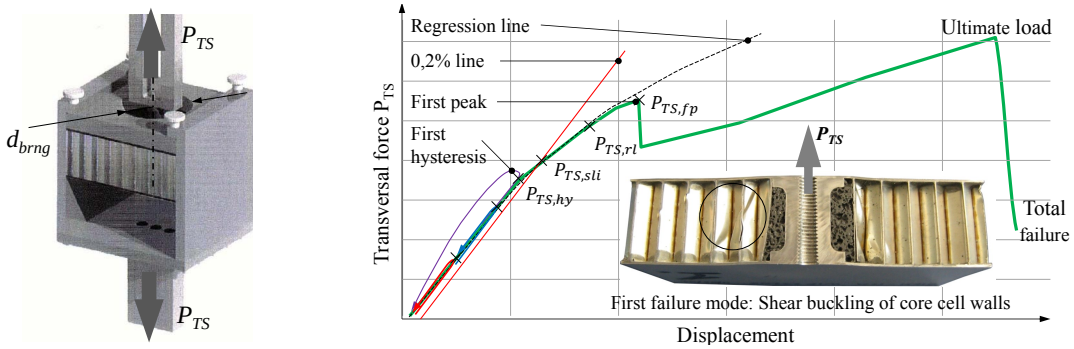

Figure 5. Failure process of an transversely loaded insert (images by [8, 48]).

An initially reversible cell wall buckling can be determined near the first local maximum of the force-deflection curve, becoming irreversible with further increasing force. This failure mechanism affects the core as well as the face sheets, Fig. 6:

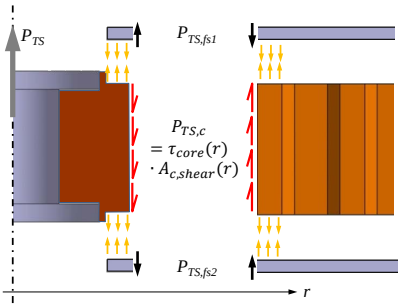

Figure 6. Load paths of a local insert load introduction subjected to transverse load.

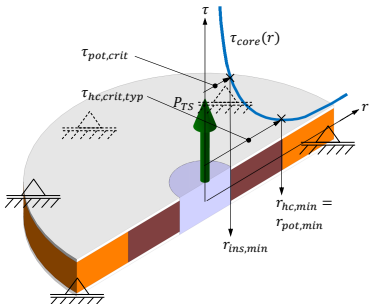

Figure 7. Minimal potting and insert radii depending on core and potting shear strength.

And therefore can be written as:

$$P_{TS} = P_{TS,c} + P_{TS,fs1} + P_{TS,fs2} \tag{1}$$

Considering only thin, flexural face sheets, their influence of their bending stiffness can be neglected [32]. Hence, the core carries almost the entire transverse load P_{TS}. For investigations regarding sandwich elements with thick, e. g. stiff face sheets see [34, 52, 53].

$$P_{TS,fs1} + P_{TS,fs2} \ll P_{TS,c} \rightarrow P_{TS,fs1}, P_{TS,fs2} \approx 0 \rightarrow P_{TS} \approx P_{TS,c}. \tag{2}$$

According to [21, 34, 48, 54], the core shear tension $\tau_{core}(r)$ is a function of the distance r, or in other words, on the ratio between the transverse load $P_{TS,c}$ and the cylindrical area $A_{c,shear}(r) = 2\pi \cdot r \cdot d_{sw}$ (with $d_{sw} = \frac{t_{fs1}}{2} + \frac{t_{fs2}}{2} + h_c$) where the shear forces acts in the sandwich core (Fig. 6, Fig. 7):

$$\tau_{core}(r) = \frac{P_{TS,c}}{2\pi \cdot r \cdot d_{sw}} \tag{3}$$

In order to prevent shear failure, the acting shear strength $\tau_{core}(r)$ must be smaller or at least equal than the shear strength of the core material $\tau_{hc,crit,typ}$:

$$\tau_{core}(r = r_{pot,otr,min}) \leq \tau_{hc,crit,typ} \tag{4}$$

Solving Eq. (3) on condition of Eq. (4), the minimum required outer potting radius $r_{pot,otr,min}$ can be calculated:

$$r_{pot,otr,min} = \frac{P_{TS,c}}{\tau_{hc,crit,typ} \cdot 2\pi \cdot d_{sw}} \tag{5}$$

Excerpt from ISBN 978-3-00-053387-7

For $\tau_{hc,crit,typ}$, ESA [31] recommends to multiply the average shear strength of the honeycomb core material in W-direction, $\tau_{W,typ}$, by a factor of 1.36:

$$\tau_{hc,crit,typ} = \tau_{W,typ} \cdot 1.36 \tag{6}$$

In this way the approximately 72% higher number of single cell walls in L- than in W-direction of honeycomb materials is recognized which is caused by the manufacturing process (Fig. 8, left). Also, the number of cells which are filled with potting resin depends on the center point position of the circular insert hole regarding to the hexagonal cells (Fig. 8, right).

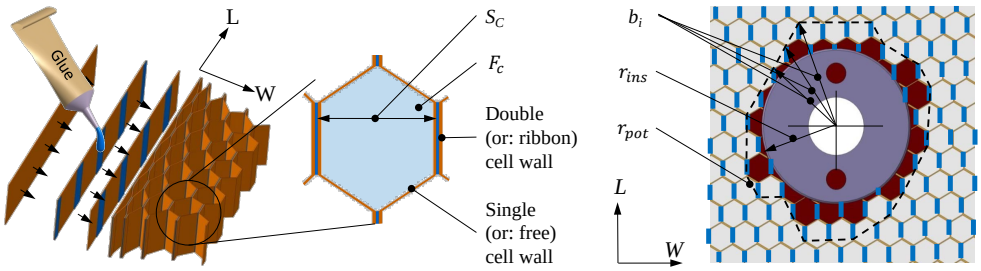

Figure 8. Unequal cell walls due to manufacturing process, parameters of the effective potting radius.

Both influencing parameters are taken into account in the effective potting radius $r_{pot,eff}$, which is an analytic dimension, describing the radial influence zone of the potting as well as the adjacent double walls. For the minimum and average $r_{pot,eff}$, ESA [31] provides equations based on empirical data, considering the honeycomb cell size S_c as well as the insert radius r_{ins}, Eq. (7), (8). As $r_{pot,otr,min}$ and $r_{pot,eff,min}$ refer to the same geometry, they can be equated (Fig. 7):

$$r_{pot,otr,min} = r_{pot,eff,min} = 0.9 \cdot r_{ins,min} + 0.7 \cdot S_c \tag{7}$$

$$r_{pot,eff,avg} = r_{ins} + 0.8 \cdot S_c \tag{8}$$

Using Eq. (5), (6) and (7) delivers the minimum insert radius $r_{ins,min}$:

$$r_{ins,min} = \frac{P_{TS,c}}{1.224 \cdot \tau_{W,typ} \cdot \pi \cdot d_{sw}} - \frac{7}{9} \cdot S_c \tag{9}$$

4. Comparison of analytic and experimental results

To proof the radius minimizing approach provided with Eq. 9, the first attempt has to be a validation of all previous presented equations. By rearranging Eq. 9, the theoretical transverse load strength $P_{TS,th}$ can be calculated:

$$\begin{aligned} P_{TS,th} &= 2\pi \cdot r_{pot,eff,min} \cdot d_{sw} \cdot \tau_{hc,crit,typ} \\ &= (\pi \cdot d_{sw} \cdot \tau_{W,typ}) \cdot (2.45\, r_{ins,min} + 1.9\, S_c) \end{aligned} \tag{10}$$

Experimental data has been taken for comparison from references [10, 45, 51, 55, 56], which include different insert load introduction shapes with different geometrical (d_{sw}, r_{ins}) and material parameter ($E_{fs}, \tau_{W,typ}$) values. The selection criteria for the reference data to be considered are, regarding the sandwich elements, thin face sheets ($\leq$ 1.5 mm) made of FRP with quasi-isotropic properties in combination with aluminum or aramid honeycomb material. The involved insert types are restricted to through-the-thickness inserts without protruding face sheet flanges (Fig. 3), table right, right column, middle type). A minimal volume of five test samples per set is accepted. For a more detailed description of the reference data see [57]. The resulting values of $P_{TS,th}$ are compared to the experimental generated transverse load strengths $P_{TS,exp}$ of the named references, offering partly high derivations up to 40%, Fig. 9.

Excerpt from ISBN 978-3-00-053387-7

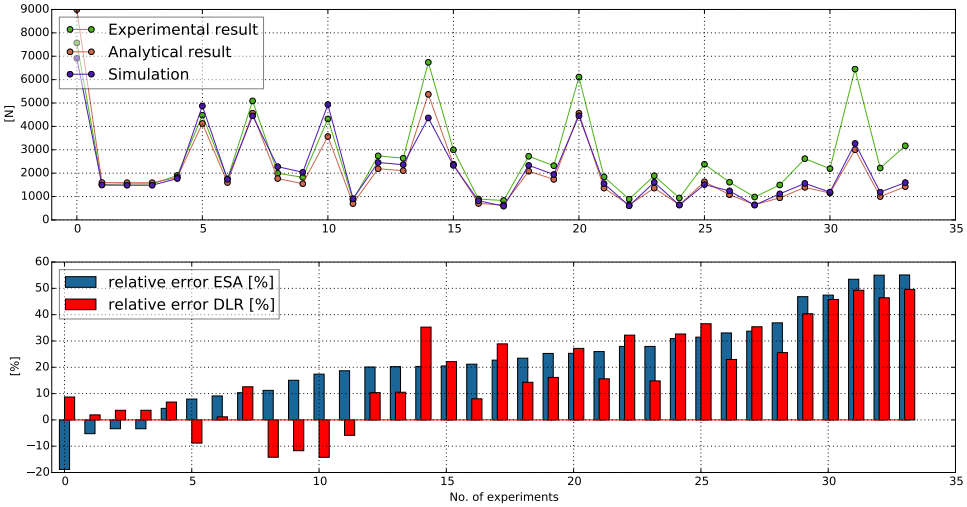

Figure 9. Comparison between analytic and experimental results.

The differences between $P_{TS,th}$ and $P_{TS,exp}$ show a high level of inaccuracy of Eq. (10). An analysis showed that the differences cannot be assigned to one particular of $d_{sw}, r_{ins}, E_{fs}, \tau_{W,typ}$ parameters [57]. Therefore, the remaining theoretical as well experimental factors of influence will be discussed in the following.

4.1. Factors influencing the analytic results: Calculation methods for $r_{pot,eff,min}$ and $\tau_{hc,crit,typ}$

ESA [31] provides a guideline to determine the effective potting radius $r_{pot,eff}$, Eq. 7. In order to investigate the stochastic behaviour of $r_{pot,eff}$, a simulation was developed. In determining $r_{pot,eff}$, the center point c_r of the potting bore-hole with respect to the honeycomb cells plays an important role as it affects the effective potting geometry [EPG] (Fig. 8, right). Due to the random behavior of c_r caused by manufacturing, its position must be considered uncertain. A Monte Carlo approach was applied in order to simulate this particular phenomenon, with the aim to determine the statistical behavior of $r_{pot,eff}$ as a function of the cell size S_c, the potting radii b_i and the random center point c_r, that is $r_{pot,eff} = f(S_c, b_i, c_r)$. An uniform distribution was applied on $c_r = \mathcal{U}(a, b)$ within the limits a and b. While $r_{pot,eff}$ may be interpreted in many ways, two different approaches were applied in this work, based on reference [31], Eq. (11) and Eq. (12). With the first approach, having the EPG, a vector b_i is constructed which spans from the center c_r to each node of the EPG. Then, $r_{pot,v}$ is the mean value of all vectors b_i, [31]:

$$b_p = \frac{1}{N} \sum_{i=1}^{N} b_i \tag{11}$$

In contrast, the real potting radius $r_{pot,R}$ is a function of the area of one cell F_c and the number of all removed or broached cells N_{pc} (Fig. 8). The entire area of removed or broached cells is given by $A_t = F_c \cdot N_{pc}$. Mapping A_t to a circle shape means $A_t = \pi \cdot b_R$, with b_R as real potting radius, thus the real potting radius reads:

$$b_R = \sqrt{\frac{N_{pc} F_c}{\pi}}. \tag{12}$$

The statistical result of the two parameters $r_{pot,v}$ and $r_{pot,R}$ shows for each insert radius r_i a different effective distribution-range:

Excerpt from ISBN 978-3-00-053387-7

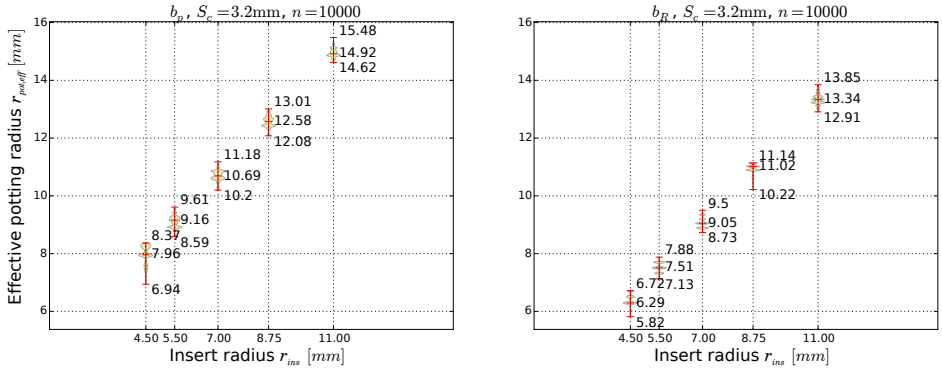

Figure 10. Statistical analyses of the simulation results for both methods $r_{pot,v}$ and $r_{pot,R}$.

The weighted mean $\bar{x} = \sum_{i=1}^{n} w_i \, b_{i(v/R)}$ with normalized weights w_i was used for the determination of the mean value of each method, $r_{pot,v}$ and $r_{pot,R}$ respectively. In order to obtain a statistical meaningful result for each insert radius r_{ins}, $n = 10000$ simulations were carried out with parameter $S_c = 3.2$ mm. A previous study showed convergence with $n \geq 1000$ simulations for each insert radius. A linear interpolation of the maximal, typical and minimal values of $r_{pot,v}$ and $r_{pot,R}$ distributions was applied to compare the data with the ESA results [31] shows a good fit in the typical range (Fig. 11, orange area and "ESA typ").

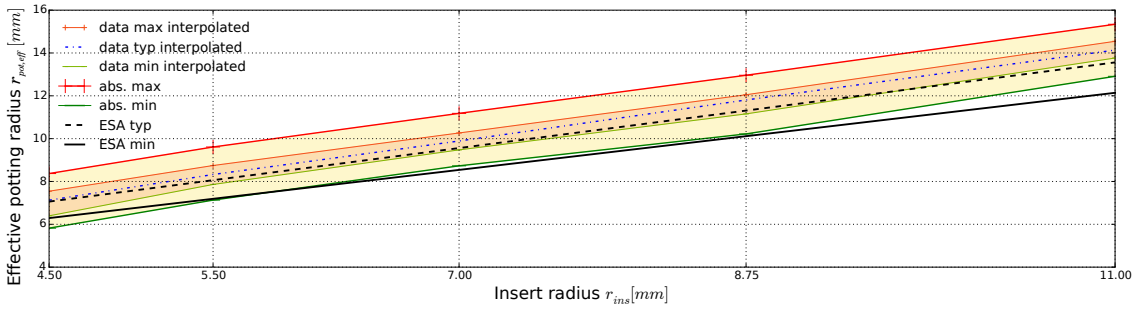

Figure 11. Comparison of DLR simulation and ESA data of the effective potting radius.

From DLR data (Fig. 11), two important linear regression function can be derived. For typical values of $r_{pot,typ}$ the interpolated data $r_{pot,v}$ and $r_{pot,R}$ (Fig. 11, orange area, "data type interpolated") can be described with $r_{pot,typ,DLR}$ (Tab. 1). The regression function with respect to the minimum values is $r_{pot,min,DLR}$. In here, only the smallest occurring values were considered. That refers to the statistical results of Eq. 12.

Table 1. Linear regression functions of the simulation data for $r_{pot,min}$ and $r_{pot,typ}$

	ESA, nonperforated core	DLR simulation
min	$r_{pot,min,ESA} = 0.9\, r_{ins} + 0.7\, S_c$	$r_{pot,min,DLR} = 1.07\, r_{ins} + 0.4\, S_c$
typ	$r_{pot,typ,ESA} = r_{ins} + 0.8\, S_c$	$r_{pot,typ,DLR} = 1.05\, r_{ins} + 0.78\, S_c$

The numerical results agree in the typical value range with a tendency of the lower limit (Fig. 11, data min interpolated). In lower range, the ESA b_{vmin} values (Fig.11, abs. min) show higher differences compared to experimental results, due to the more conservative approach of the ESA estimation of $r_{pot,eff}$.
Regarding the calculation of the typical shear strength of honeycomb material $\tau_{hc,crit,typ}$, Eq. (6) by ESA [31] is not trusted due to a lack of derivations of the factor 1.36 as well as why to use $\tau_{W,typ}$. To prove whether the results match best with the different shear strength values in L- and W-direction, $\tau_{L,typ}$, $\tau_{L,min}$, $\tau_{W,typ}$ or $\tau_{W,min}$, the theoretical core shear strength $\tau_{typ,theo}$ is calculated by merging Eq. (3) and (6) and comparing the results, Eq. (13) resp. Fig. 12. The factor 1.36 as well as the usage of $\tau_{W,typ}$

Excerpt from ISBN 978-3-00-053387-7

fits well and therefore Eq. (6) can be recommended.

$$\tau_{typ,theo} = \frac{P_{TS,exp}}{2\pi \cdot r_{pot,eff,min} \cdot d_{sw} \cdot 1.36} \tag{13}$$

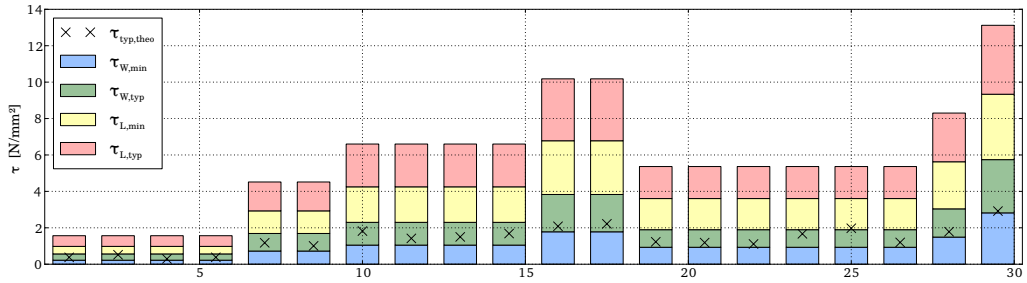

Figure 12. Comparison of honeycomb shear strength values of recalculated and experimental data.

Considering the negligence of face sheet influence, Eq. (2), no literature is familiar to the authors defining the maximal bending stiffness of the face sheets whether the influence of the face sheets is no more negligible. However, the stiffer the face sheets, the more load is transported by them, discharging the honeycomb core.

4.2. Factors influencing the experimental results: Test and evaluation methods for $\tau_{W,typ}$ and $P_{TS,exp}$

Values of honeycomb shear buckling strength in W-direction, $\tau_{W,typ}$ depends highly on the testing method used (ASTM C 273, DIN 53294, double lap shear test as well as three-point beam shear test, [58, 59]). Unfortunately, the information in data sheets [60–62] are limited as they contain neither information about the used shear test method nor sample number. Therefore, own honeycomb shear tests, applying statistically meaningful sample sizes, are evident for a precise determination of $\tau_{W,typ}$.
Due to no existing testing standards for insert load introductions, the considered literature references used various test rig arrangements ranging from rigs with twosided, straight lined bearing supports [8, 56], to circular bearing supports with divergent diameters ($d_{brng} = 35 - 140$ mm), (Fig. 5 left), [11, 16, 21, 23, 24, 30, 35, 47, 49–51]. Regarding the derivation of $P_{TS,exp}$ from experimental raw data, the considered literature references provide four different methods: Either using the first peak value of the load-displacement curve (Fig. 5, right, $P_{TS,fp}$, [8, 10, 23, 45, 48, 50]), an intersection with a 0.2 or 5% straight line ($P_{TS,sli,0.2}$, [47, 63]), an intersection with a regression line ($P_{TS,rl}$, [49]) as well as a determination by a hysteresis procedure ($P_{TS,hy}$, [24, 35]). The hysteresis test approach is recommended for providing the most precise values and may be extended by acoustical determination.

5. Conclusions

The overall objective of this work is to generate a fast sizing tool, adapting the shape of insert elements to the respective mechanical conditions as basis for lightweight load introductions in sandwich elements. For the determination of the minimal radius of the inserts central cylinder, an analytic equation, given by [21, 34, 48, 54] is used. Within a first validation attempt, experimental data was taken from various literature references and compared to the equation results, yielding occasional high differences. The reason can be addressed to a large quantity of uncertainty factors, in particular to geometrical and material parameters as well as testing- and evaluation methods. By an elimination of the uncertainty of the minimal potting radius with a Monte Carlo simulation, the scatter of the theoretical influence factors could be reduced. For further reduction, investigations will focus on own, standardized tests as well as data evaluation methods and the integration of the bending stiffness of the facings into the equation. In progress of uncertainty quantification not only the test values, but also their statistic distribution is important.

Excerpt from ISBN 978-3-00-053387-7

References

[1] A. Starlinger. *Bemessen von Sandwichbauteilen*. Stadler Rail Group, Zürich, 2008.

[2] Forschungsprogramm Mobilität Bundesamt für Energie BFE, editor. *Entwicklung einer Karosserie in Sandwich-Plattenbauweise für ein Elektrofahrzeug, Schlussbericht*. Bern, 2010.

[3] M. Hertrich. Leicht und crashsicher geklebt. *adhäsion KLEBEN & DICHTEN*, 59(1-2):16–19, 2015.

[4] F. Campbell. *The Case Against Honeycomb Core*. Boeing, AMR&D Phantom Works, Long Beach, Kalifonien, USA, 2004.

[5] J.S. Kim, S.J. Lee, and K.B. Shin. Manufacturing and structural safety evaluation of a composite train carbody. *Composite structures*, 78(4):468–476, 2007.

[6] H.Y. Ko, K.B. Shin, K.W. Jeon, and S.H. Cho. A study on the crashworthiness and rollover characteristics of low-floor bus made of sandwich composites. *Journal of mechanical science and technology*, 23(10):2686–2693, 2009.

[7] C. Berggreen, C. Lundsgaard-Larsen, K. Karlsen, C. Jenstrup, and B. Hayman. Improving performance of polymer fiber reinforced sandwich X-joints in naval vessels. Technical report, Technical University of Denmark, Department of Mechanical Engineering, 2007.

[8] J. Block, T. Brander, M. Lambert, J. Lyytinen, K. Marjoniemi, R. Schütze, and L. Syvänen. Carbon fibre tube inserts-a light fastening concept with high load carrying capacity. In *Spacecraft Structures, Materials and Mechanical Testing 2005*, volume 581, page 133, 2005.

[9] J.Y. Choi, K.I. Song, J.H. Choi, K.S. Kim, Y.S. Jang, and J.H. Kweon. An investigation on the strength of insert joints of composite-honeycomb sandwich structures. *Composites Research*, 20(5):26–33, 2007.

[10] K.I. Song, J.Y. Choi, J.H. Kweon, J.H. Choi, and K.S. Kim. An experimental study of the insert joint strength of composite sandwich structures. *Composite structures*, 86(1):107–113, 2008.

[11] H.C. Davies, M. Bryant, M. Hope, and C. Meiller. Design, development, and manufacture of an aluminium honeycomb sandwich panel monocoque chassis for formula student competition. *Proceedings of the Institution of Mechanical Engineers, Part D: Journal of Automobile Engineering*, page 0954407011418578, 2011.

[12] S. Milton and S.M. Grove. Composite sandwich panel manufacturing concepts for a lightweight vehicle chassis. *ACMC, University of Plymouth*, 1997.

[13] Zollkriminalamt Köln. Leitfaden Zollsichere Herrichtung von Straßenfahrzeugen und Behältern mit wärmegedämmten Aufbau. *Loseblattsammlung. [Guideline]*, pages S. 1 – 148, 2005.

[14] H.K. Cho, J.K Seo, B.J. Kim, T.S. Jang, W.H. Cha, D.G. Lee, and N.H. Myung. Development of a composite spacecraft structure for STSAT-3 satellite program. *Journal of the Korean Society for Aeronautical & Space Sciences*, 38(7):727–736, 2010.

[15] B.J. Kim and D.G. Lee. Development of a satellite structure with the sandwich T-joint. *Composite Structures*, 92(2):460–468, 2010.

[16] J.W. Lim and D.G. Lee. Development of the hybrid insert for composite sandwich satellite structures. Technical report, 2011.

Excerpt from ISBN 978-3-00-053387-7

[17] C.I. Grastataro, T.A. Butler, B.G. Smith, and T.C. Thompson. Development of a composite satellite structure for FORTE. Technical report, Los Alamos National Lab., NM (United States), 1995.

[18] A. Zinno, A. Prota, E. Di Maio, and C.E. Bakis. Experimental characterization of phenolic-impregnated honeycomb sandwich structures for transportation vehicles. *Composite Structures*, 93(11):2910–2924, 2011.

[19] J. Winter, J. König, G. Kopp, and H. Dittus. Next generation train. The revolution. *Railvolution*, 4:28–37, 2012.

[20] J. Wolff. Nutzung gefalteter Sandwichstrukturen als tragendes Bauteil mit integrierter Medienführung. *Institut für Land- und Seeverkehr Fachgebiet Kraftfahrzeuge TU Berlin und Institut für Fahrzeugkonzepte FK-LHB Deutsches Zentrum für Luft- und Raumfahrt e.V.*, 2007.

[21] S. Heimbs and M. Pein. Failure behaviour of honeycomb sandwich corner joints and inserts. Technical report, Composite Structures 89, 2009.

[22] Hexcel S.A. The basics on bonded sandwich construction TSB 124 1981 revision. *Hexcel S.A*, 1981.

[23] G. Bianchi, G.S. Aglietti, and G. Richardson. Optimization of bolted joints connecting honeycomb panels. Technical report, University of Southampton, School of Engineering Sciences, 2006.

[24] P. Bunyawanichakul, B. Castanie, and J.J. Barra. Non-linear finite element analysis of inserts in composite sandwich structures. Technical report, Composites: Part B 39, 2008.

[25] Shur-Lok Company. Fasteners for sandwich structure catalog. Technical report, 1999.

[26] The Young Engineers Inc. Engineering standard inserts cross reference list. Available at `www.youngengineers.com`, 2014.

[27] Witten Company Inc. Witten fasteners high performance fasteners and hardware products. Available at `www.wittenco.com`, 2009.

[28] RUAG Schweiz AG RUAG Space. Automating inserts for sandwich panels. Composites World, Vol. 9. *Germany : Gardner Business Media*, 2015.

[29] B. Dale. Outer space: The final frontier is exciting again! *Knoxville USA Institute for Advanced Composites Manufacturing Innovation IACMI. Composites World.*, 2015.

[30] B.J. Kim and D.G. Lee. Characteristics of joining inserts for composite sandwich panels. *Composite Structures*, 86(1):55–60, 2008.

[31] ESA-ESTEC. *Space Engineering Insert Design Handbook*, volume ECSS-E-HB-32-22A. Noordwijk, Niederlande, 2011.

[32] O.T. Thomsen. Analysis of sandwich plates with through-the-thickness inserts using a higher-order sandwich plate theory. 1994.

[33] N. Raghu, M. Battley, and T. Southward. Strength variability of inserts in sandwich panels. *Journal of Sandwich Structures and Materials*, 11(6):501–517, 2009.

[34] E. Bozhevolnaya, A. Lyckegaard, O.T. Thomsen, and V. Skvortsov. Local effects in the vicinity of inserts in sandwich panels. *Composites Part B: Engineering*, 35(6):619–627, 2004.

[35] P. Bunyawanichakul, B. Castanie, and J.J. Barrau. Experimental and numerical analysis of inserts in sandwich structures. *Applied composite materials*, 12(3-4):177–191, 2005.

Excerpt from ISBN 978-3-00-053387-7

[36] D. Keller, G. Kress, and P. Ermanni. Evolutionary strength optimization of onsert and insert shapes for local load introduction. *CIMNE-Konferenz, Barcelona*, 2007.

[37] B. Smith and B. Banerjee. Reliability of inserts in sandwich composite panels. *Composite Structures*, 94(3):820–829, 2010.

[38] D. Keller, G. Kress, and P. Ermanni. Evolutionary strength optimization of onsert and insert shapes for local load introduction. 2007.

[39] J. Jakobsen, J.H. Andreasen, O.T. Thomsen, and E. Bozhevolnaya. Fracture mechanics modelling and experimental meassurements of crack kinking at sandwich core-core interfaces. *Sandwich Construction 8: Icss 8*, 2008.

[40] C. Burchardt. Fatigue of sandwich structures with inserts. *Composite structures*, 40(3):201–211, 1997.

[41] Y. Frostig, M. Baruch, O. Vilnay, and I. Sheinman. High-order theory for sandwich-beam behavior with transversely flexible core. *Journal of Engineering Mechanics*, 118(5):1026–1043, 1992.

[42] O.T. Thomsen and W. Rits. Analysis and design of sandwich plates with inserts - a high-order sandwich plate theory approach. *Composites Part B: Engineering*, 29(6):795–807, 1998.

[43] V. Skvortsov and O.T. Thomsen. Analytical estimates for the stresses in face sheets of sandwich panels at junctions between different core materials. In *Proceedings of the 6th International Conference on Sandwich Structures (icss-6)*, 2003.

[44] B. Banerjee and B. Smith. The Thomsen model of inserts in sandwich composites: An evaluation. *arXiv preprint arXiv:1009.5431*, 2010.

[45] J. Block. Study on carbon fibre tube inserts, summary report. Technical report, Deutsches Zentrum für Luft- und Raumfahrt e.V. Institut für Strukturmechanik. Braunschweig, Germany, 2004.

[46] G.Kress and P.Ermanni. The onsert: A new joining technology for sandwich structures. Technical report, Zürich, 2004.

[47] R. Roy, K.H. Nguyen, Y.B. Park, J.H. Kweon, and J.H Choi. Testing and modeling of nomex^{TM} honeycomb sandwich panels with bolt insert. *Composites Part B: Engineering*, 56:762–769, 2014.

[48] G. Bianchi, G.S. Aglietti, and G. Richardson. Static performance of hot bonded and cold bonded inserts in honeycomb panels. *Journal of Sandwich Structures and Materials*, 2010.

[49] R. Seemann and D. Krause. Virtual testing of nomex honeycomb sandwich panel inserts. *20th International Conference on Composite Materials.*, 2015.

[50] K.H. Nguyen, Y.B. Park, J.H. Kweon, and J.H. Choi. Failure behaviour of foam-based sandwich joints under pull-out testing. *Composite Structures*, 94(2):617–624, 2012.

[51] Y.B. Park, J.H. Kweon, and J.H. Choi. Failure characteristics of carbon/BMI-Nomex sandwich joints in various hygrothermal conditions. *Composites Part B: Engineering*, 60:213–221, 2014.

[52] E. Bozhevolnaya and A. Lyckegaard. Local effects at core junctions of sandwich structures under different types of loads. *Composite Structures*, 73(1):24–32, 2006.

[53] K.K.U. Stellbrink. Krafteinleitungen in Faserkunststoffverbunden. Technical report, Technische Universität Stuttgart. Germany, 2006.

Excerpt from ISBN 978-3-00-053387-7

[54] J.P. Cushman and R.J. Murphy. Geometric considerations in the design of honeycomb sandwich fasteners. *Journal of Spacecraft and Rockets*, 3(11):1686–1688, 1966.

[55] J. Block. Study on carbon fibre tube inserts, synthesis of analysis and tests. Technical report, Deutsches Zentrum für Luft- und Raumfahrt e.V. Institut für Strukturmechanik. Braunschweig, Germany, 2007.

[56] Buderus Sell GmbH, G.W. Seeburger, and H.J. Schetat. Design values report, panel inserts, d0-001-120e. Technical report, Herborn, 1993.

[57] J. Wolff, F. Trimpe, R. Zerlik, and C. Hühne. Evaluation of an analytical approach prediciting the transversal failure load of insert connections in sandwich structures. *20th International Conference on Composite Materials, ICCM 20*, 2015.

[58] A.J. Hodge and A.T. Nettles. A novel method of testing the shear strength of thick honeycomb composites. 1991.

[59] H.G. Allen. *Analysis and Design of Structural Sandwich Panels: The Commonwealth and International Library: Structures and Solid Body Mechanics Division*. Oxford : Pergam Press, 1969.

[60] *HexWeb Honecomb Sandwich Design Technology*. Duxford, 2000.

[61] Germany Plascore GmbH & CoKG. PN2 aerospace grade aramid fiber honeycomb. Available at `www.plascore.de`, 2015.

[62] Germany Schütz GmbH & Co. KGaA. Selters. Coremaster C1 Technische Daten. Available at `www.schuetz.net`, 2015.

[63] J. Block. Technical note 4, test report. Technical report, Inst. FA Deutsches Zentrum für Luft- und Raumfahrt DLR. Carbon Fibre Tube Inserts (Part 2). Braunschweig, Germany, 2007.

Excerpt from ISBN 978-3-00-053387-7